

Extracting Anomalous Gluon-Top-Quark Effective Couplings at the Supercolliders

D. Atwood, A. Aeppli, and A. Soni

Department of Physics, Brookhaven National Laboratory, Upton, New York 11973

(Received 30 March 1992)

Production of $t\bar{t}$ by gluon fusion followed by $t \rightarrow bW^+$, $\bar{t} \rightarrow bW^-$, and $W^\pm \rightarrow e^\pm \nu_e(\bar{\nu}_e)$ is studied to extract the CP -violating chromoelectric dipole moment form factor of the top quark. The fact that the spin of the top quark, in its rest frame, is in the direction of the e^+ momentum facilitates the analysis. Expressions for the differential cross section and decays are given. We find that at the Superconducting Super Collider or CERN Large Hadron Collider, it is possible to put a limit of $10^{-20}g_s$ to $10^{-19}g_s$ cm on these effective couplings through the use of "optimal observables." Naive observables such as simple triple product correlations are typically an order of magnitude less effective.

PACS numbers: 14.80.Dg, 12.38.Bx, 13.40.Fn, 13.85.Qk

Although the top quark has not been discovered yet, study of the physics of the top quark may well be the most important task which the Superconducting Super Collider (SSC) performs. Current bounds on the mass (m_t) of the top quark are 89 GeV [1] $\leq m_t \leq 180 \text{ GeV}$ [2], in which case the SSC or the CERN Large Hadron Collider (LHC) will produce 10^7 to 10^8 $t\bar{t}$ pairs [3] per year. From the theoretical point of view, the fact that the top quark has such a large mass compared to the five lighter quarks suggests that it may be susceptible to effects from TeV-scale physics not readily observable in lighter quarks.

Among the properties of the top quark which should be measured at the SSC are its basic couplings to gauge bosons. In this paper we investigate the possibility of extracting the effective couplings of the top quark to the gluon through the observation of correlations between the t and \bar{t} polarizations in hadronic collisions. These correlations are extracted by studying the decay products of the t and \bar{t} . We find that such couplings may be measured with sufficient precision to serve as useful constraints on some extensions to the standard model.

We generalize the effective Lagrangian for top-quark-gluon interaction to include terms of dimension 5:

$$L_C = \frac{1}{2} \frac{\mathcal{C}}{m_t} \bar{t} \sigma^{\mu\nu} F_{\mu\nu}^i T_i t, \quad L_D = \frac{i}{2} \frac{\mathcal{D}}{m_t} \bar{t} \sigma^{\mu\nu} \gamma_5 F_{\mu\nu}^i T_i t, \quad (1)$$

where $\sigma^{\mu\nu} = \frac{1}{2} i[\gamma^\mu, \gamma^\nu]$, $F_{\mu\nu}^i$ is the gluon field strength, and $T_i = \frac{1}{2} \lambda_i$, $i=1, \dots, 8$. The coefficient C ($-\mathcal{C}/m_t$) in the term L_C is then referred to as the "chromomagnetic" dipole moment (CMDM), which as in the case of QED, receives one-loop contributions in QCD which will be of the order $g_s \alpha_s / \pi m_t$. This would very likely mask any contributions to C due to new physics. On the other hand D ($=\mathcal{D}/m_t$), the "chromoelectric" dipole moment (CEDM), violates CP . A nonvanishing value for it would be a strong indication of new physics. We will therefore focus on the measurement of D .

In general, of course D (and likewise C) are form factors (i.e., functions of momentum transfer). Terms in the effective Lagrangian which give rise to such momentum dependence of D are of dimension greater than 5. Thus,

for our purposes we neglect them. Indeed in model calculations the real part of the form factors are constant to a good approximation [4].

In the standard model (SM), the coefficient C can arise at the one-loop level in QCD whereas D only receives a contribution at three or more loops in electroweak interactions and is expected to be very small ($\leq 10^{-30}g_s$ cm) [5]. In some of the extensions of the SM [4], D , in particular, can be much larger than in the SM. For example, in models with CP nonconservation through Higgs boson exchange [6] D may be about $10^{-20}g_s$ cm [4]. This is many orders of magnitude larger than the EDM for light quarks (or the neutron) expected in extensions of the SM [7,8].

In hadronic collisions at the SSC, $t\bar{t}$ pairs are made predominantly through the gluon-gluon fusion diagrams show in Figs. 1(a)-1(c). If we introduce the interactions L_C and L_D , we also must include the Feynman diagram 1(d) due to the non-Abelian terms in $F_{\mu\nu}$ (i.e., to preserve gauge invariance).

We assume here that the couplings $C, D \ll g_s/m_t \approx 10^{-16}g_s$ cm are small enough that we are justified in expanding the matrix element squared to first order in C, D . Below we give this matrix element squared for $gg \rightarrow t\bar{t}$ to first order in C and D where we have averaged over initial gluon polarization but kept the explicit top-quark polarizations. We denote the initial gluon momenta by p_{g1} and p_{g2} , the momentum and spin of the \bar{t} by p_{t1}

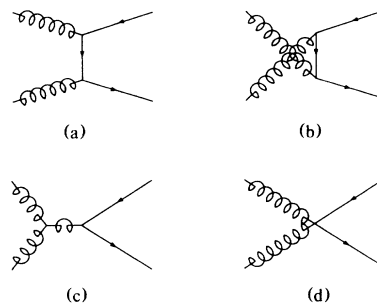


FIG. 1. Tree-level Feynman diagrams for $gg \rightarrow t\bar{t}$. The diagram in (d) is needed to preserve gauge invariance.

and S_{i1} , respectively, and the momentum and spin of the \bar{t} by p_{i2} and S_{i2} . In terms of these we define the following:

$$Q = p_{g1} + p_{g2}, \quad P_i = p_{i1} - p_{i2}, \quad P_g = p_{g1} - p_{g2}, \quad R^\mu = P_i^\sigma Q^\rho P_g^\tau \epsilon_{\sigma\rho\tau}^\mu, \quad (2)$$

where $\hat{s} = Q^2$. We also define

$$r = \left(\frac{\hat{s} - 4m_t^2}{\hat{s}} \right)^{1/2}, \quad z = -\frac{P_i \cdot P_g}{\hat{s}r}, \quad \rho = \frac{2}{\hat{s}^2} (R \cdot S_{i1} P_g \cdot S_{i2} - [1 \leftrightarrow 2]),$$

$$\beta = \frac{2}{\hat{s}^2} (R \cdot S_{i1} P_i \cdot S_{i2} - [1 \leftrightarrow 2]), \quad \gamma = \frac{4}{\hat{s}} P_g \cdot S_{i1} P_g \cdot S_{i2}, \quad \tau = \frac{4}{\hat{s}} P_i \cdot S_{i1} P_i \cdot S_{i2}, \quad (3)$$

$$\eta = \frac{2}{\hat{s}} (P_i \cdot S_{i1} P_g \cdot S_{i2} + [1 \leftrightarrow 2]), \quad \xi = 2S_{i1} \cdot S_{i2}.$$

Thus to first order in C, D the spin and color matrix element squared is

$$\frac{1}{256} \sum_{\text{gluons}} |M|^2 = \frac{g_s^4}{64} \left[H_0 + \frac{C}{g_s} H_C + \frac{D}{g_s} H_D \right], \quad (4)$$

where

$$H_0 = \frac{9r^2 z^2 + 7}{6(r^2 z^2 - 1)^2} \{ [r^4(z^4 - 2z^2 + 2) - 2r^2 + 1] \xi - (z^2 - 1)r^2(\gamma + \tau - 2zr\eta) - 2[z^4 r^4 + 2r^2(1 - r^2)z^2 + 2r^4 - 2r^2 - 1] \},$$

$$H_C = -\frac{(1 - r^2)^{1/2} \sqrt{\hat{s}}}{3(r^2 z^2 - 1)^2} [14(z^2 r^2 - 1)\xi + (9z^2 r^2 + 7)(z^2 - 1)r^2 \gamma + (9r^4 z^2 + 5r^2 z^2 + 7r^2 - 21)\tau$$

$$- (9r^2 z^2 - 9r^2 + 16)(z^2 r^2 - 1)zr\eta + 4(9z^2 r^2 + 7)(z^2 r^2 - 1)], \quad (5)$$

$$H_D = \frac{(1 - r^2)^{1/2} \sqrt{\hat{s}}}{3(1 - z^2 r^2)^2 (1 - z^2)} \{ [9r^4 z^6 - r^2(18r^2 - 7)z^4 + (18r^4 - 25r^2 + 16)z^2 + 7(2r^2 - 3)] \rho + \frac{z}{r} (1 - z^2 r^2)(9r^2 + 5)\beta \}.$$

This expression agrees with [9] when summed over polarization.

One can see from these expressions that in order to detect D , one needs to have information about the polarization of the top quark. Fortunately, the left-handed nature of the weak decay allows us to determine the top-quark polarization quite easily. Consider the decay chain $t \rightarrow bW^+ \rightarrow be^+ \nu_e$. In the limit that the mass of the b quark can be ignored, the properties of the weak interaction force all the particles in the final state to be left handed. Thus, the amplitude for top-quark decay is proportional to kinematic factors times

$$\bar{u}_b \gamma_\mu (1 - \gamma_5) u_t \bar{u}_e \gamma^\mu (1 - \gamma_5) \nu_e. \quad (6)$$

If we apply a Fierz transformation to the above we get

$$\frac{1}{2} \bar{u}_b (1 + \gamma_5) u_e^c \bar{\nu}_e^c (1 - \gamma_5) u_t. \quad (7)$$

where $u^c = C\bar{u}^T$, C being the charge conjugation matrix. This implies that the spin of the top quark, S_{i2} , is in the direction of the positron momentum in the top-quark rest frame. Thus Eq. (5) in fact gives the matrix element for the complete process $gg \rightarrow t\bar{t}$ including the subsequent semileptonic decay chain of the top quark.

Consider now the hadronic decay chain $t \rightarrow bW^+ \rightarrow b\bar{q}q'$. The situation is the same as the above except that the S_{i2} is in the direction of the \bar{q} . Experimentally, however, it may not be possible to distinguish between the quark and the antiquark jets. Thus, the experimentally

observed polarization is the average over these two possibilities.

In a related work [10] we showed how an optimal observable can be chosen so as to maximize the precision for measuring a given parameter. To illustrate this let us denote the differential cross section by

$$\Sigma(\Phi) d\Phi = \hat{\sigma}(x_1 x_2 s) f_g(x_1) f_g(x_2) dx_1 dx_2 d\phi,$$

where x_1 and x_2 are the gluon momentum fractions, f_g is the gluon structure function, $\hat{\sigma} d\phi$ is the subprocess differential cross section, and ϕ is the final-state phase space and we define $d\Phi = d\phi dx_1 dx_2$. We now expand this differential cross section in the quantity which we wish to observe, denoted as λ (thus, for example, $\lambda = D$):

$$\Sigma(\Phi) d\Phi = [\Sigma_0(\Phi) + \lambda \Sigma_1(\Phi)] d\Phi. \quad (8)$$

The optimal observable to measure λ is given by

$$f_{\text{opt}}(\Phi) = \Sigma_1(\Phi) / \Sigma_0(\Phi), \quad (9)$$

where f_{opt} has the property that it maximizes the precision for measuring λ as compared to any other observable. Using Eq. (4) we see that $f_{\text{opt}} = H_D / g_s H_0$. Note also that f_{opt} shares the same symmetry properties as Σ_1 [10]; in the case of the CEDM it will thus be CP odd.

In a realistic hadronic collider, of course, not all of the momenta which enter into the problem are immediately observable. Consider the overall process of top-quark

production followed by the semileptonic decay of $t\bar{t}$. In this case neutrino momenta are not observed; neither are the longitudinal momenta of the initial gluons. The neutrino momenta p_ν and \bar{p}_ν may, however, be indirectly determined if we assume that the electron and b jets are well measured since the eight unknown components of the neutrino momenta are constrained by the following eight equations:

$$p_\nu^2 = \bar{p}_\nu^2 = 0, \quad (p_\nu + p_{e^+})^2 = (\bar{p}_\nu + p_{e^-})^2 = m_W^2, \quad (p_\nu + p_{e^+} + p_b)^2 = m_t^2, \tag{10}$$

$$(\bar{p}_\nu + p_{e^-} + \bar{p}_b)^2 = m_t^2, \quad (p_\nu + p_{e^-} + p_b + \bar{p}_\nu + p_{e^+} + \bar{p}_b)_{\text{transverse}} = 0.$$

The solution of these equations, however, gives rise to a twofold or fourfold ambiguity which must be considered.

At the SSC [11], we take the collision energy to be $\sqrt{s} = 40$ TeV and the yearly luminosity to be 10^4 pb^{-1} . The calculation [3] gives the cross section for $pp \rightarrow t\bar{t}$ to be 25 nb for $m_t = 100$ GeV and 6 nb in the case of $m_t = 200$ GeV. This corresponds to 1.2×10^7 "leptonic" $t\bar{t}$ pairs (i.e., where both the W bosons decay leptonically, lepton = e or μ) in the case of $m_t = 100$ GeV and 0.3×10^7 such pairs when $m_t = 200$ GeV. In order to avoid the uncertainty in these cross sections due to the structure functions and acceptance cuts which may be present in a specific detector, we will present our results in terms of 1σ limits on the CEDM assuming a sample of 10^7 leptonic $t\bar{t}$ pairs. We find that results calculated in this way vary by only a few percent with changes in structure functions or changing from the SSC $\sqrt{s} = 40$ TeV to the LHC $\sqrt{s} = 16$ TeV. The limits given a different sized sample of events may be calculated by scaling $\lambda_{\min} \propto N^{-1/2}$, where λ_{\min} is the 1σ limit obtained and N is the number of events.

In Fig. 2 we show the precision of the CEDM that can be achieved as a function of m_t at the SSC assuming 10^7 leptonic $t\bar{t}$ pairs. For definiteness, we used the EHLQ-2 structure functions [12] for these plots. The lower solid curve shows the case for the optimal observable. In order to take into account the reconstruction ambiguity mentioned above, we also considered a modified optimized observable defined by

$$f' = \sum_i \Sigma_1(\Phi_i) / \sum_i \Sigma_0(\Phi_i), \tag{11}$$

where the sum is over the different possible reconstructions. Once again f' shares the symmetry properties of f or of Σ_1 . This operator leads to the limit shown by the dotted curve. Comparison with the lower solid curve readily reveals that the reconstruction ambiguity does not cause any significant changes in the attainable limit.

In addition to the optimal observables we also considered the limits which may be obtained by using various simply defined observables, for example, triple products of momenta. The best limit that we were able to obtain was for the observable

$$f_1 = \rho / \hat{s}. \tag{12}$$

Again we take into account the ambiguity discussed above and in Fig. 2 we show f'_1 , where

$$f'_1 = \sum_i f_1 f_g(x_1) f_g(x_2), \tag{13}$$

with the long-dashed curve. Note that this is almost a factor of 2 worse than the optimal observable.

Since the optimal observables are fairly complicated entities, their use may entail new systematic errors. We therefore also consider simple observables which may be constructed exclusively out of momenta which are directly observed. In Fig. 2 the long-dash-dotted curve shows the limits obtained for the observable

$$f_2 = \frac{\epsilon_{\mu\nu\sigma\rho} p_{e1}^\mu p_{e2}^\nu p_{b1}^\sigma p_{b2}^\rho}{(p_{e1} \cdot p_{e2} p_{b1} \cdot p_{b2})^{1/2}}, \tag{14}$$

which involves both lepton and quark momenta. The upper solid curve shows the limits for

$$f_3 = (p_{e1}^x p_{e2}^y - p_{e1}^y p_{e2}^x) \text{sgn}(p_{e1}^z - p_{e2}^z) (p_{e1} \cdot p_{e2})^{1/2}, \tag{15}$$

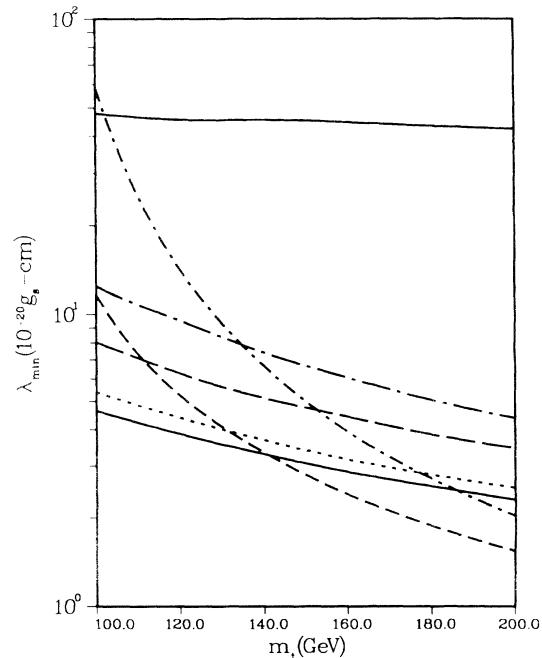


FIG. 2. Attainable 1σ limits, in units of $10^{-20} g_s^{-1} \text{ cm}$ on the CEDM normalized to 10^7 leptonic $t\bar{t}$ events: the optimal observable for a leptonic $t\bar{t}$ pair (the lower solid curve), for a leptonic $t\bar{t}$ pair averaged over the reconstruction ambiguity (dotted curve), with a leptonic-hadronic $t\bar{t}$ (short-dashed curve), and for a hadronic $t\bar{t}$ pair (short-dash-dotted curve), and the CEDM observable f_1 (long-dashed curve), the CEDM observable f_2 (long-dash-dotted curve), and the CEDM observable f_3 (upper solid curve).

where $\text{sgn}(x) = +1$ for $x \geq 0$ and -1 for $x < 0$. This observable, which is similar to those considered in [13], is dependent only on the lepton momenta so although it provides limits an order of magnitude less stringent than those considered above, it is easiest to determine experimentally.

The energy asymmetry between (say) the charged leptons, i.e.,

$$a_E = \frac{\langle E_+ \rangle - \langle E_- \rangle}{\langle E_+ \rangle + \langle E_- \rangle}, \quad (16)$$

is also CP violating and can be readily used (see Refs. [14,15]). However, this observable [unlike the triple correlation (15)] is even under "naive T " and consequently it requires D in Eq. (1) to have an imaginary part. Such an imaginary part must, however, vanish at zero momentum transfer so this form factor must be related to terms in the effective Lagrangian of dimension greater than 5 and is therefore not being considered in this paper.

It is also useful to consider what limits may be obtained when one or both of the W bosons decay hadronically. In this case we are not subject to the type of reconstruction ambiguity which occurs in the pure leptonic case. We are, however, subject to the ambiguity due to the difficulty in distinguishing the quark and the anti-quark jet. Again to obtain the optimal observable we define f' as in Eq. (11) where the sum this time is taken over this twofold (in the case of one leptonic top quark and one hadronic) or fourfold uncertainty (in the case both top quarks decay hadronically). Note that due to the branching ratio of the W boson, our basic sample of 10^7 leptonic $t\bar{t}$ pairs implies a sample of 6×10^7 leptonic-hadronic $t\bar{t}$ pairs and 9×10^7 hadronic $t\bar{t}$ pairs.

The short-dashed curve in Fig. 2 shows the limit using f' in the leptonic-hadronic case and the short-dashed-dotted curve shows the limit obtained using f' in the hadronic case. As can be seen the leptonic-hadronic type of event may be the best for larger top-quark masses (≥ 150 GeV) but at the expense of some increment in experimental difficulties. We thus see that depending on the assumptions made, D may be measured to a precision of $5 \times 10^{-20} g_s$ to $10^{-18} g_s$ cm.

Note that with respect to the CEDM all the observables which we consider above are CP odd; hence QCD will not contribute at any order through the subprocess $gg \rightarrow t\bar{t}$. However, the overall process at the SSC is $p + p \rightarrow t\bar{t} + X$ with an initial state that is not a CP eigenstate. Hence there is no guarantee that these operators will not in fact receive a QCD contribution at higher orders.

Within the framework of the parton model, these operators will only receive a contribution if the initial state contains two valence quarks. The simplest such process is $q_v q_v \rightarrow q_v q_v t\bar{t}$ (q_v is a u or d valence quark). In addition there must be a loop since the tree-level diagram is essentially a gluon-gluon collision. We may estimate,

therefore, that the contribution to a CP -violating operator from this background will correspond to a CEDM of

$$\frac{\alpha_s^3}{\pi^3} \frac{d\hat{L}_{q_v q_v}(\hat{s})}{d\hat{L}_{gg}(\hat{s})} \frac{g_s}{m_t},$$

where $d\hat{L}_{q_v q_v}$ and $d\hat{L}_{gg}$ are the differential luminosities for $q_v q_v$ and gg , respectively. Using the values for \hat{L} at $m_t \approx \hat{s} \approx 150$ GeV from [12] we find that the level of this background corresponds to a CEDM of $\approx 10^{-23} g_s$ cm, well below the level which could be seen at the SSC.

Summarizing, we find that the chromoelectric-dipole moment of the top quark may be measured to a precision ranging from about $5 \times 10^{-20} g_s$ to $10^{-18} g_s$ cm. Insofar as the CEDM may be $\sim 10^{-20} g_s$ cm, in some extensions of the SM, for example, in models with extra Higgs bosons [4], one may therefore expect this type of measurement to begin to put some constraints on such models.

This manuscript has been authored under Contract No. DE-AC02-76CH00016 with the U.S. Department of Energy.

-
- [1] CDF Collaboration, F. Abe *et al.*, Phys. Rev. D **45**, 3921 (1992).
 - [2] W. J. Marciano, BNL Report No. 45999, 1991 (to be published).
 - [3] S. Dawson and S. Godfrey, Phys. Rev. D **39**, 221 (1989).
 - [4] A. Soni and R. M. Xu, Phys. Rev. Lett. **69**, 33 (1992).
 - [5] J. Donoghue, Phys. Rev. D **18**, 1632 (1978); E. P. Shabalin, Yad. Fiz. **31**, 1665 (1980) [Sov. J. Nucl. Phys. **31**, 864 (1980)]; I. Khriplovich and M. Pospelov, INP Novosibirsk Report No. 90-123, 1990 (to be published).
 - [6] S. Weinberg, Phys. Rev. Lett. **37**, 657 (1976); T. D. Lee, Phys. Rev. D **8**, 1226 (1973); for a recent review, see H. Y. Cheng, Int. J. Mod. Phys. A **7**, 1057 (1992).
 - [7] See, for example, D. Atwood *et al.*, Phys. Lett. B **256**, 472 (1991), and references therein.
 - [8] For a general review of the electric dipole moment of light fermions, see W. Marciano, in *BNL Summer Study of CP Violation*, edited by S. Dawson and A. Soni (World Scientific, Singapore, 1990); S. Barr and W. Marciano, in *CP Violation*, edited by C. Jarlskog (World Scientific, Singapore, 1989), p. 455; W. Bernreuther and M. Suzuki, Rev. Mod. Phys. **63**, 313 (1991).
 - [9] R. K. Ellis and J. C. Sexton, Nucl. Phys. **B282**, 642 (1987).
 - [10] D. Atwood and A. Soni, Phys. Rev. D **45**, 2405 (1992).
 - [11] Particle Data Group, J. J. Hernández *et al.*, Phys. Lett. B **239**, 1 (1990).
 - [12] E. Eichten, I. Hinchliffe, K. Lane, and C. Quigg, Rev. Mod. Phys. **56**, 579 (1984).
 - [13] A. Aeppli and A. Soni, Phys. Rev. D **46**, 315 (1992); W. Bernreuther and O. Nachtmann, Phys. Rev. Lett. **63**, 2787 (1989); **64**, 1072 (1990); W. Bernreuther, G. W. Botz, O. Nachtmann, and P. Overmann, Z. Phys. C **52**, 567 (1991); G. Kane, G. Ladinski, and C. P. Yuan, Phys. Rev. D **45**, 124 (1992).
 - [14] G. Valencia and A. Soni, Phys. Lett. B **263**, 517 (1991).
 - [15] The energy asymmetry is also used by C. R. Schmidt and M. E. Peskin, Phys. Rev. Lett. **69**, 410 (1992).